Structural Health Monitoring of Wind Turbine Blades[*]

Mark A. Rumsey[†] and Joshua A. Paquette[‡]
Sandia National Laboratories[§], Albuquerque, NM 87185

ABSTRACT

As electric utility wind turbines increase in size, and correspondingly, increase in initial capital investment cost, there is an increasing need to monitor the health of the structure. Acquiring an early indication of structural or mechanical problems allows operators to better plan for maintenance, possibly operate the machine in a de-rated condition rather than taking the unit off-line, or in the case of an emergency, shut the machine down to avoid further damage. This paper describes several promising structural health monitoring (SHM) techniques that were recently exercised during a fatigue test of a 9 meter glass-epoxy and carbon-epoxy wind turbine blade. The SHM systems were implemented by teams from NASA Kennedy Space Center, Purdue University and Virginia Tech. A commercial off-the-shelf acoustic emission (AE) NDT system gathered blade AE data throughout the test. At a fatigue load cycle rate around 1.2 Hertz, and after more than 4,000,000 fatigue cycles, the blade was diagnostically and visibly failing at the out-board blade spar-cap termination point at 4.5 meters. For safety reasons, the test was stopped just before the blade completely failed. This paper provides an overview of the SHM and NDT system setups and some current test results.

Keywords: wind turbine blades, Fatigue Testing, Acoustic Emission, Macro-Fiber Composite

1. STATE OF WIND ENERGY TECHNOLOGY

In 2007, 5,244 megawatts (MW) of electric generation from wind energy was installed in the United States. This expanded the nation's total wind power generating capacity by 45% in a single calendar year, and injected an investment of over $9 billion into the economy. These new wind power projects accounted for about 30% of all new electric utility power-producing capacity added nationally in 2007. The U.S. wind power fleet can now generate 16,818 MW and spans 34 states.[1,2] Worldwide the installed capacity is 94,112 MW.[3,4] American wind farms will generate an estimated 48 billion kilowatt-hours of wind energy in 2008, just over 1% of U.S. electricity supply, powering the equivalent of over 4.5 million homes. A typical electric utility wind turbine being installed today can exceed 1.5 MW of rated output power, and the trend is toward even larger turbines.[5] See Figure 1. (A one-MW wind turbine can generate as much electricity as 250 to 300 average U.S. homes use.[6])
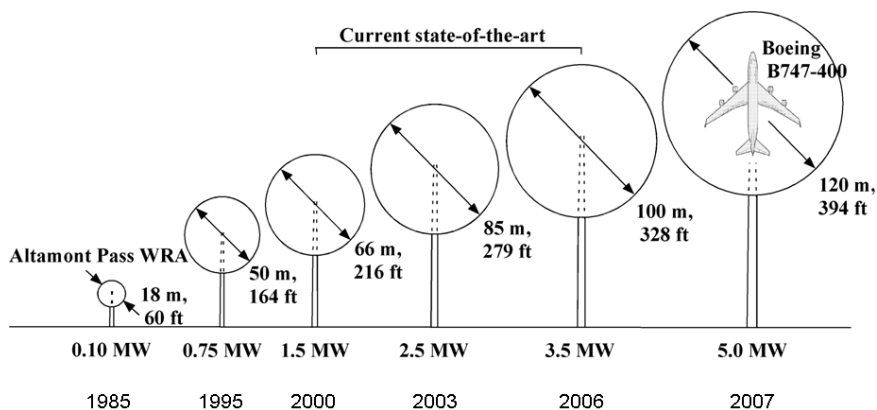

Figure 1: The trend in wind turbine size is to grow larger.

---

2. INTRODUCTION

As utility-size wind turbines increase in size, and correspondingly their initial capital investment cost, there is an increasing need to monitor the health of these structures. Acquiring an early indication of structural or mechanical problems allows operators to better plan for maintenance, possibly operate the machine in a de-rated condition rather than take the turbine off-line, or in the case of an emergency, shut the machine down to avoid further damage.

Numerous damage detection, condition and structural health monitoring devices, techniques and algorithms exist for a whole host of structures.[7,8,9,10,11] This paper, however, focuses on the SHM and NDT techniques that were applied during a fatigue test of a wind turbine blade. The specifics of each SHM and NDT technique used will be individually described in the Fatigue Test Setup section that follows. The blade on a typical utility-size wind turbine, typically constructed of fiberglass, can exceed 40 meters in length and weigh over 7 tons, and like the wind turbine, the trend in blades is toward larger, longer and heavier blades. While the capital cost of a wind turbine has gone up, the cost of energy has come down.[12]

In 2002, Sandia National Laboratories (SNL) initiated a research and development program to demonstrate the use of carbon fiber in subscale wind turbine blades.[13,14,15] From this effort, SNL created three 9 meter designs with assistance from Global Energy Concepts[16], Dynamic Design Engineering[17], and MDZ Consulting[18]. From each blade design, seven blades (a total of 21 blades) were manufactured by TPI Composites.[19,20] All blades were designed for a 100-kilowatt stall-controlled turbine, a wind turbine SNL utilizes for field testing.[21]

The second blade design, the TX-100 (Twist-bend Experimental), was designed to have passive aerodynamic load reduction by orienting unidirectional carbon fiber at an optimum angle of 20° off the pitch axis in the skins.[22,23,24,25,26,27] The TX-100 blade also contained a fiberglass spar cap that terminated at 4.5 meters, mid-span in the blade. It was determined that the large amount of carbon contained in the skin was adequate to carry loads outboard in this design, making a full-length spar cap unnecessary. A simplified drawing of the planform of the TX-100 blade is shown in Figure 2. The area of the blade skin containing carbon fiber is shown in blue, and the unidirectional fiberglass spar cap is shown in red.
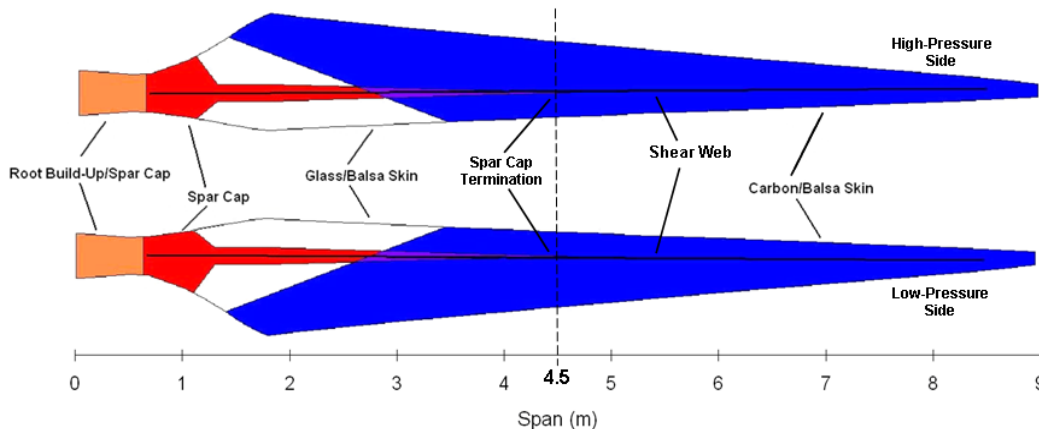

Figure 2. – Diagram showing major structural elements in the TX-100 wind turbine blade.

In support of the SNL blade research and development program, a comprehensive set of tests was defined. The results from a series of static blade tests have already been reported.[28] The particular test described in this paper was a fatigue test of a TX-100 wind turbine blade, to blade failure. The primary goal of the test was to acquire a fatigue dataset that would be used to help validate the blade design and structural computer codes,[29] and to provide feedback in the blade design and manufacturing process. However, fatigue testing a pristine newly manufactured blade over the full life cycle of the blade also provides a unique opportunity to exercise structural health monitoring (SHM) and Nondestructive Testing (NDT) systems in a laboratory environment. The objectives of this fatigue test were to:
1. Determine structural properties of the blade through fatigue testing,
2. Determine fatigue strength and failure mode of the blade,
3. Investigate new sensor technologies for damage detection and structural health monitoring.

3. FATIGUE TEST SETUP

3.1 Test Specimen
The test specimen was TX-100 wind turbine blade #002. The blade was 9.0 meters (29.5 feet) long and weighed 160.5 kg (354.0 pounds).

3.2 Test Location
The fatigue test was performed at the National Wind Technology Center (NWTC)[30], a laboratory within the National Renewable Energy Laboratory (NREL)[31] complex. The NREL headquarters is located in Golden, Colorado. The NWTC is located south of Boulder, Colorado. The blade fatigue testing was performed in the highbay in building A60.

3.3 Test Fixture Hardware and Blade Structural Loading
The blade was bolted to a 1,360 kiloNewton-meter (1,000 foot-kilopounds) test stand in a cantilever and approximate horizontal orientation with the low-pressure blade surface facing down. Figure 3 shows a photo of the test area.
The fatigue test was planned such that the blade would fail sometime between 1 and 4 million cycles. The oscillating
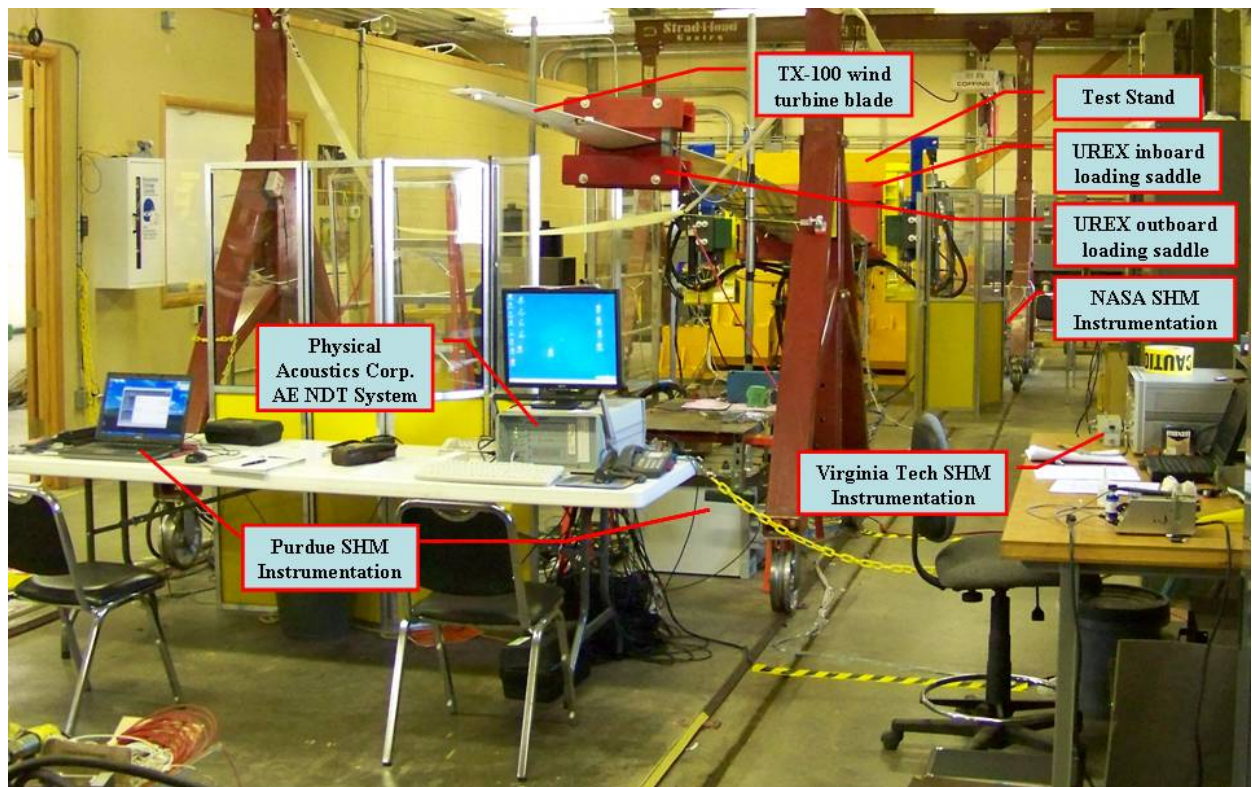

Figure 3 – Photo of the blade fatigue test area.

load was calculated and prescribed to simulate the cyclical loading that the blades would see in a 20-year field operation, but at an accelerated damage level. The loading was developed by taking into consideration the results of the previously completed static test along with the standard values used to calculate fatigue of the material components of the blade carbon/epoxy and glass/epoxy.[28]

Fatigue cycles were induced in the blade by using a novel resonant system called the Universal Resonance Exciter (UREX). The UREX system consisted of a hydraulically driven mass, weighing 620 kg (1360 lb), mounted approximately at 1.6 meters from the blade root, at approximately maximum blade chord, and an outboard mass weighing 180 kg (390 lb) mounted at the 6.75 meter station. The UREX was driven to excite the first flap frequency and induce a cyclic load in the blade. The applied moment range was controlled by adjusting the frequency and stroke of the UREX. Adjustments were made automatically by the UREX controller based on the feedback signal of an accelerometer

that was placed on the blade tip. From time to time manual adjustments were made to the frequency if the blade frequency had changed due to temperature effects. The test frequency varied around 1.2 Hertz (Hz), and with the occasional stops for blade inspection and other static tests, the test could run from 1 to 2 months.

All the equipment on the blade (UREX, sensors, actuators, cables) was weighed prior to the fatigue testing. This was the tare load. The mass of the blade was not included in the tare load. A further detailed discussion of the UREX, fatigue test setup, and model validation process can be found in reference 32.

The blade was loaded with a reversal ratio, R=0.1, with the low-pressure down-facing surface in constant compression.[33] For the first 1 million cycles, the maximum load corresponded to a root moment of approximately 31% of that which caused failure in the static test. This load level was predicted to cause failure in 4 million cycles. Starting at 1 million cycles, the load was increased in 10% increments and every 500k cycles thereafter. The target and applied test loads for the first load step and the applied test load for the static test are shown in Figure 4.
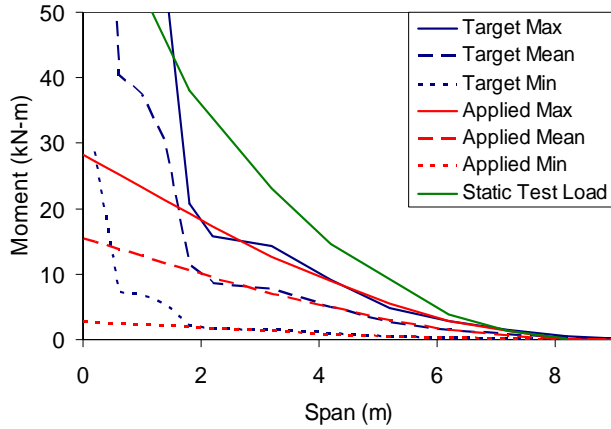
No load cell was used during the test. Instead a calibration pull was performed on the blade and the strain was measured at the root. The load was then calculated from the strain seen at the root. The output from strain gage G5 (see Figure 5) was connected to a signal conditioner to provide an amplified high-level output signal and was made available to the other test parties as the derived load level.

Figure 4 – Calculated UREX fit of 4-million-cycle target load for TX-100 fatigue test.

Ambient temperature near the blade root was continuously measured throughout the test.
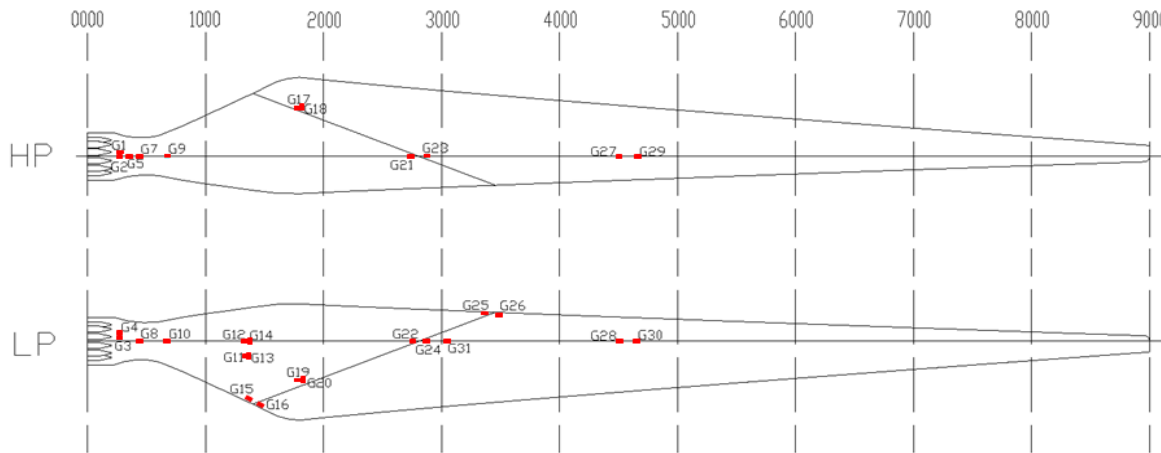

Figure 5 – Diagram showing the layout of strain gages.

3.4 Possible Blade Failure Mechanism and Location

To strategically place the SHM sensors, we needed to know the TX-100 blade failure mechanism in fatigue and the failure location, however, neither of which were known. Our only previous experience with this blade design was a TX-100 static test to blade failure and the blade failed between 1 and 3 meters from the root, near maximum chord, on the compression side. In the previous static test of a TX-100 blade, failure was dominated by structural characteristics rather than material weakness. Furthermore, previous fatigue tests of other similar 9-meter blades have resulted in failure in the transition region of the blade near maximum chord. Using this information, we recommended the SHM sensors be placed around the maximum chord area and on the compression side of the blade. For this test setup, the compression side would be facing down toward the floor.

3.5 Strain gages

Thirty 1000-ohm metal foil strain gages were installed on the gel-coat surface of the blade in a layout as shown in Figure 5. The strain gages were zeroed at the flapwise tare load. Detailed information about the strain gauge locations and orientations is given in reference 32.

3.6 Physical Acoustics Corporation Acoustic Emission (AE) NDT System

The Physical Acoustics Corporation[34] (PAC) acoustic emission NDT system was setup by Dr. Alan Beattie[35] and Dr. Adrian Pollock[36].

The acoustic emission sensors specifically monitor sound waves that propagate on the blade surface. These sound waves are often caused by structural damage (that is, fiber breakage, delamination, disbonding) occurring in the blade.

During preliminary tests, acoustic velocity and attenuation measurements were made by placing two PAC AE sensors 0.15 meters apart on a section of the TX-100 blade and doing ten pencil lead breaks 0.05 meters behind each sensor. The vectors between the two sensors were oriented at angle increments of ten degrees from the blade axis. For the frequency response of R6I sensors, the attenuations lay between 0.02 and 0.10 dB/mm. This corresponds to a spread in attenuation of 8 to 40 dB between sensors for the maximum chosen separation of 0.4 meters.

Twenty-four PAC Model R6I AE sensors were mounted on the blade surface over critical areas and interfaces inside the blade. The sensor layout shown in Figure 6 was determined on site after the acoustic characteristics had been measured. (Sensor #25 was not used during the fatigue test.) A PAC DiSP system using PAC AEwin software acquired and processed the AE signals. Much of the data processing was done by custom programs, developed by Beattie, because of the high acoustic anisotropy and variability produced by the diverse material characteristics, orientations and interfaces of the internal components of the blade.
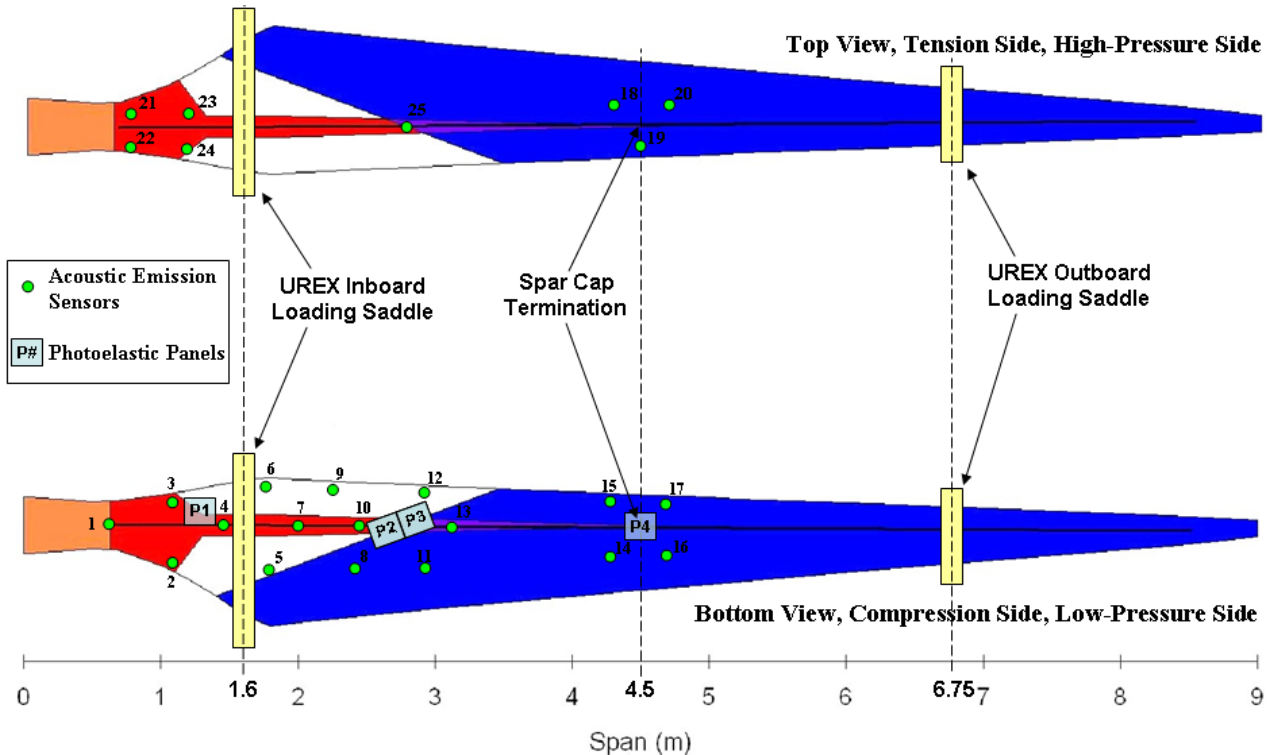

Figure 6 – Layout of the acoustic emission NDT sensors and photoelastic panels.

3.7 NASA Kennedy Space Center SHM System

Rudy Werlink[37], with NASA Kennedy Space Center, implemented a wave propagation based SHM technique by instrumenting the high-pressure side of the blade with a Macro-Fiber Composite (MFC) actuator and three MFC sensors, and on the low-pressure side an MFC actuator and two MFC sensors. His setup was an incremental enhancement, with the application of the electronic filter, to the setup on previous wind turbine blade tests.[38] The actuators were Smart Material[39] MFC, model 8557-S1, 3.375 x 2.25 inches in size. The sensors were Smart Material MFC, model 5-21, were 1.5 x 1 inches in size. The actuator/sensors needed to encompass the expected failure area. Close-up photos of the NASA sensor arrays are shown in Figure 7.
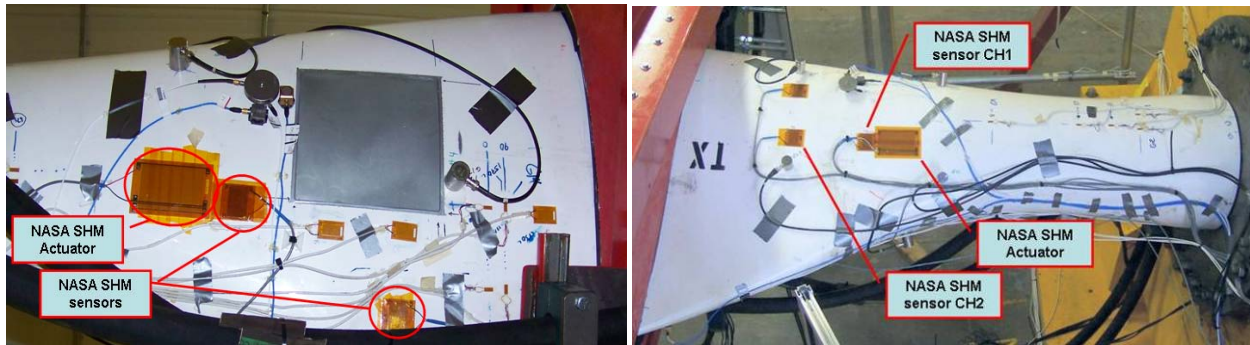

Figure 7 – Photos of the NASA SHM sensor arrays. The left photo shows the low-pressure (downward facing) side of the blade. The right photo shows the high-pressure (upward facing) side of the blade. The larger MFC patches were used as actuators, the smaller MFC patches were used as sensors.

Both actuators were energized with a random-frequency input signal. The timeseries data was collected for 30-seconds in the following sequence of configurations:

1. Up-side array actuated with the blade load not cycling.
2. Up-side array actuated with blade load cycling, and using an electronic filter on the sensor output to reduce the self-generated voltages resulting from the reaction of the blade while resonating.
3. Down-side array actuated with blade load not cycling.
4. Down-side array actuated with blade load cycling, and using the sensor output filter.

As in the previous blade tests, NASA provided all the SHM equipment except the data acquisition system (DAS). Data from the MFC sensors was collected by a SNL ATLAS[40,41,42] at a sample rate of 5,000 Hz. After the initial system checkout, NREL testing staff operated the SNL ATLAS, exercised the NASA SHM system, acquired the data, and posted the data on a secure NREL FTP file server to allow remote file access by the testing partner.

3.8 Purdue University SHM System

The Purdue University test team was lead by Jonathan White[43] under the guidance of his Professor Doug Adams[44]. Purdue provided all the SHM instrumentation, test equipment and data acquisition systems, and rotated one to two staff members in and out of the NREL NWTC test site over the duration of the test.

Sensor placement was determined ahead of time using the results from pre-testing on a 15-foot cantilevered helicopter rotor blade recently erected at the Herrick Laboratories at Purdue University.[45] An array of high sensitivity triaxial accelerometers, low-frequency capacitive accelerometers, and piezoelectric actuators with force sensors was distributed over the surface of the blade to monitor the loading and blade damage. A triaxial accelerometer at the tip was used to measure the tip deflection in the flap, lead-lag, and root-tip directions throughout the test. A few photos of the Purdue SHM setup are shown in Figure 8.

Prior to the start of the fatigue test, a modal analysis of the blade in the flap-wise direction was performed. The SHM approach implemented the restoring force method, a passive structural health monitoring algorithm, using 4-each PCB 3711D1FA20G and 4-each PCB 3711D1FA50G triaxial accelerometers. The method of virtual forces, transmissibility and other time-frequency analysis techniques, active structural health monitoring algorithms, was also applied with 4-each PCB 712A02 actuators, 4-each PCB 208C01 force sensors and 4-each PCB 356B18 triaxial accelerometers. The

Purdue test team also recorded passive response measurements throughout the test when the blade was under fatigue loads. More details of the Purdue instrumentation setup are given in reference 46.
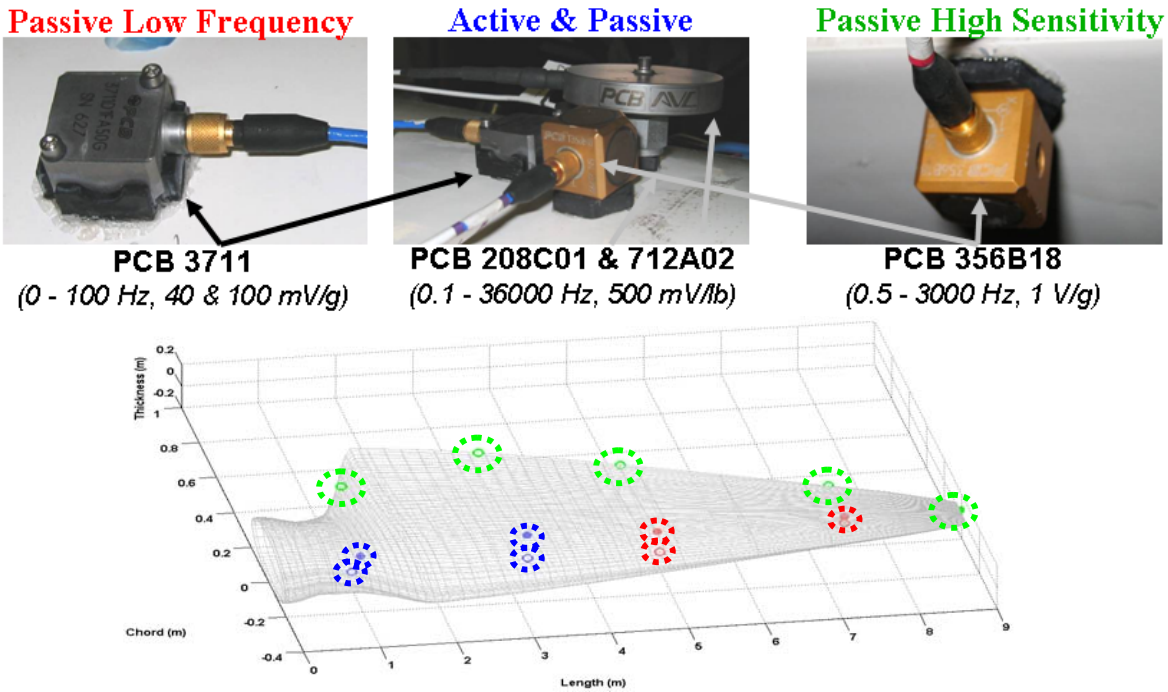

Figure 8 – Layout and some photos of the accelerometers used in the Purdue SHM system. (Accelerometers indicated with solid dots were on the upper high-pressure side of the blade, those with open dots on the lower low-pressure side.)

3.9 Virginia Tech SHM System

The Virginia Tech (VT) test team was lead by Corey Pitchford[47] under the guidance of Professor Dan Inman[48]. The VT impedance-based SHM system consisted of 6-each Smart Material MFC self-sensing actuators, model M2814-P1, mounted on the blade surface and an Agilent HP4192A impedance analyzer. The instrumentation setup can be seen in Figure 9. Initially for this test it was desired to use an Analog Devices, Inc., AD5933 Impedance to Digital Converter integrated circuit to measure the impedance. Unfortunately, problems arose getting the AD5933 to produce acceptable real impedance results so an Agilent HP4192A impedance analyzer was used in its place. Preliminary tests back at VT on a CX-100 wind turbine blade section showed that using MFC sensors on the blade in place of PZTs and mounting the MFCs on the outside of the blade instead of the inside caused less structural information to show up in the impedance, but damage was still detected. The HP4192A was shipped to NWTC for the fatigue test, along with a laptop running the Piezoelectric Resonance Analysis Program (PRAP) software, version 2.1, to control the impedance analyzer and record data. The switchbox (the blue box shown in Figure 9) was built so that all six MFCs could be connected to the impedance analyzer simultaneously, and then one could be selected at a time to be the input. This greatly simplified the routine for collecting impedance data.

A description of the VT impedance-based SHM technique is presented in greater detail in reference 49.

Figure 9 – Setup of the Virginia Tech SHM instrumentaton.

The MFCs were all bonded on the low-pressure (downward-facing) side of the blade between 1 and 3 meters from the root. Failure was expected in this area from modeling and previous similar tests.[28] The locations within this area were chosen based on the internal geometry of the blade. The blade geometry along with the sensor locations is illustrated in Figure 10. Figure 11 shows two photos of the MFCs bonded to the wind turbine blade, 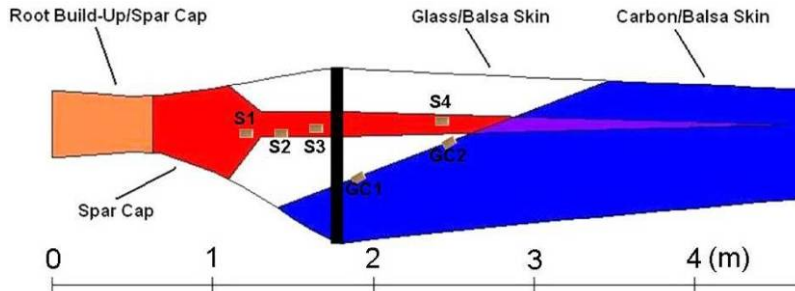along with many other sensors used during the fatigue test. Failure was expected near the spar cap close to the 1 meter area, so three MFCs were mounted in this area and were named S1, S2, and S3. One additional MFC was mounted on the spar cap region near the intersection of the spar cap, glass/balsa skin, and carbon/balsa skin and was named S4. Finally, two MFCs were mounted on the glass/balsa and carbon/balsa intersection on the skin, one at about 2 meters, GC1, and one near the spar cap and carbon fiber interface, GC2.
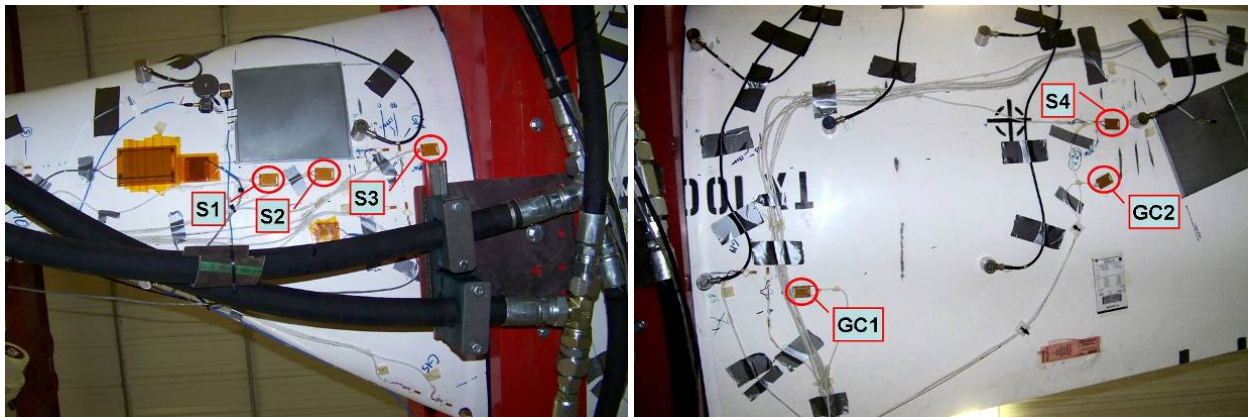

Figure 10 – Diagram showing layout of Virginia Tech sensor array.

Figure 11 – Photos showing the Virginia Tech SHM sensor arrays. The self-actuating sensors S1, S2, S3, S4, GC1 and GC2 are circled in red.

3.10 Miscellaneous Instrumentation

Four 8 inch by 8 inch photoelastic panels were applied on the low-pressure (downward-facing) side of the blade surface over key locations in the blade as shown in Figure 6. Three of the four photoelastic panels are visible in the photos shown in Figure 11. The photoelastic panels were used to provide a qualitative evaluation of the load/strain paths.

Two FLIR ThermaCAM infrared thermography cameras, models P60 and SC640, were used at various times to monitor and obtain snapshots of thermal gradients and hot-spots as the fatigue test progressed.

3.11 Test Procedure

All strain gages on the blade and the ambient temperature near the blade root were monitored continuously throughout the fatigue test. At least once a day the fatigue test was stopped by halting the UREX to acquire datasets for the NASA, Purdue and VT SHM systems, and to inspect the blade for any damage. There was unacceptable interference between the active SHM diagnostic systems, so each SHM system had to be exercised in sequence to avoid cross-talk interference. Periodically, the NREL testing staff would post test data, photos and log files on a secure NREL FTP file server to allow remote file access by the testing partners.

4. RESULTS

4.1 Blade Failure scenario and mechanism

The TX-100 blade fatigue test started on July 19, 2007, and ended October 23, 2007, at 4,001,558 fatigue cycles. Starting at about 700,000 cycles, a multitude of fine gel-coat cracks developed on the high-pressure (upward facing) side the blade running at an angle of 65 degree with respect to the spanwise axis. The cracks were most apparent in the 4.0 to 5.6 meter span of the blade. The 65 degree angle coincides with the principal axis of the ±45-degree fiberglass laminate that is a constituent of the carbon/glass triax material used in the blade skins. As these gel coat cracks progressed in length and gap width, from 723,000 cycle count to 2.4 million cycle count, the principal axis of the crack front changed from 65 degrees to 20 degrees, which is the same angle as the principal direction of the carbon fiber in the blade skins. At about 2.5 million cycles, a larger visible crack developed parallel to the chord axis on the high-pressure (upward facing) side, near the 4.5 meter station. The crack then grew along the 20 degree off-pitch-axis carbon fiber direction until the test was stopped at 4 million cycles because of excessive torsional motion of the blade tip and an accelerated growth rate in crack length. Figure 12 shows the high-pressure (upward facing) surface damage above the spar cap skin interface at the 4.5 meter station.

The incipient cause of damage, and the resultant failure in the TX-100 blade, was a stress riser at the spar cap termination point at the 4.5 meter station.
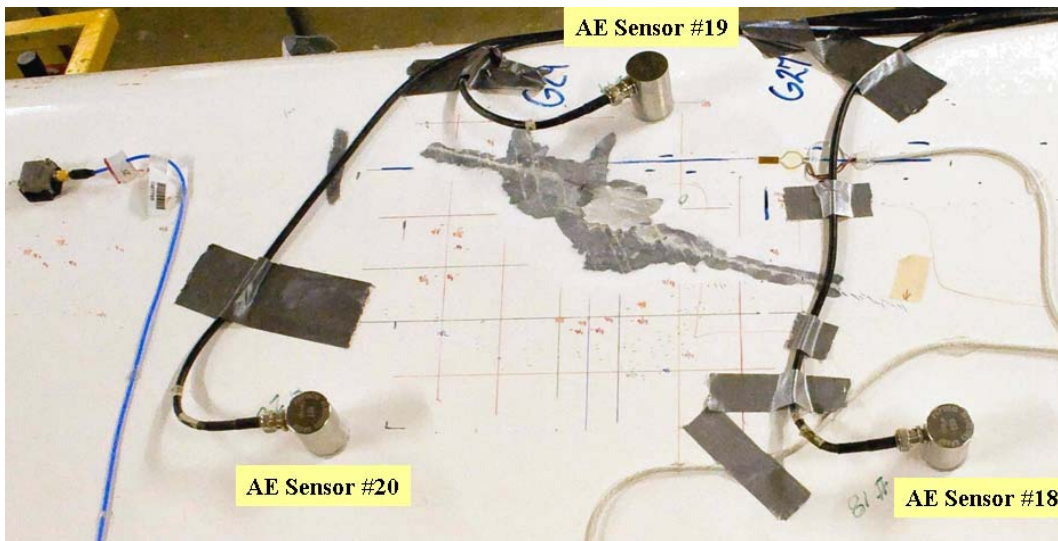
4.2 NDT and SHM Results

Figure 12 – Photo showing the blade surface around the area of failure. Some of the gel-coat has been manually removed to better evaluate the underlying damage in the fiberglass and carbon fiber laminate.
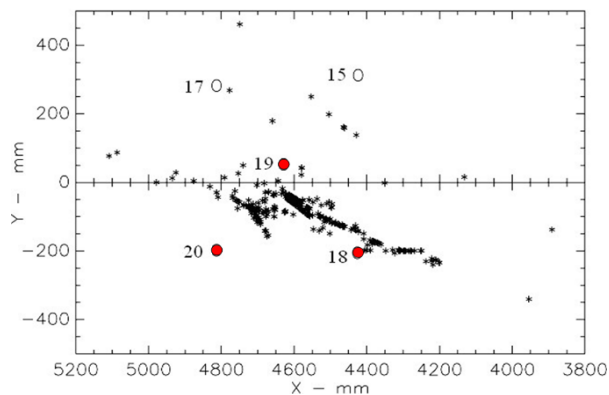

Figure 13 – Map of the acoustic emission events on the blade.

Soon after the fatigue test started, the PAC AE NDT system received significant AE events around AE sensors 18, 19 and 20, and then clearly followed the evolution of blade failure. The acoustic emission data showed damage accumulating on the high-pressure (upward-facing) surface around the end of the spar cap at 4.5 meters, with no significant damage in any of the other monitored areas. Significant damage did not appear until about 3.55 million cycles and extreme damage started at 3.78 million cycles. Compare the AE events shown in Figure 13 to the visual damage shown in Figure 12.

The AE parameter used to indicate damage was a measure of the detected acoustic energy emitted per cycle in the damaged region. To determine the intensity of the emission, the true energy of the waveforms was used. Once the acoustic waveform was digitized, the true energy was easy to measure. It is simply the sum of the product of the square of each digitized voltage times the digitization interval over the entire length of the transient signal. Knowing the input impedance of the preamplifier allows the calculation of the energy. In PAC DiSP energy units, the calibration of N units is $E = Nx0.000931$ milli-attoJoules or $E = Nx6.7041x10^{-6}$ million-electron-Volts (MeV). The rate of generation of acoustic energy can be obtained from the slope of the summed energy versus time curves. Knowing the frequency of blade cycling gives the acoustic energy generation rate in MeV/cycle. For most of the test, this rate was less than 0.01 MeV per cycle. At the point of peak damage, this rate went up to 30 MeV per cycle. See Figure 14 and Figure 15.
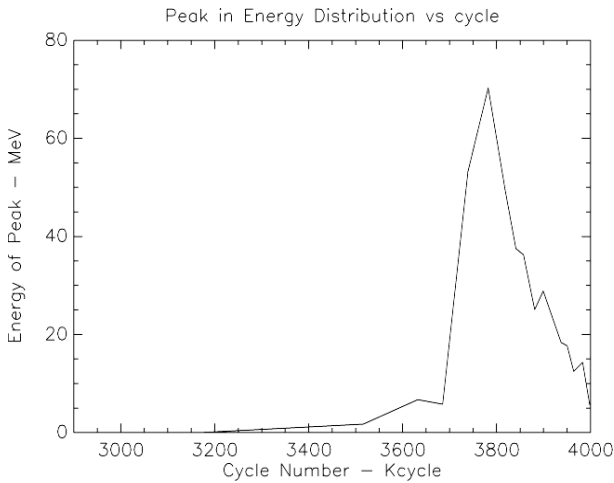

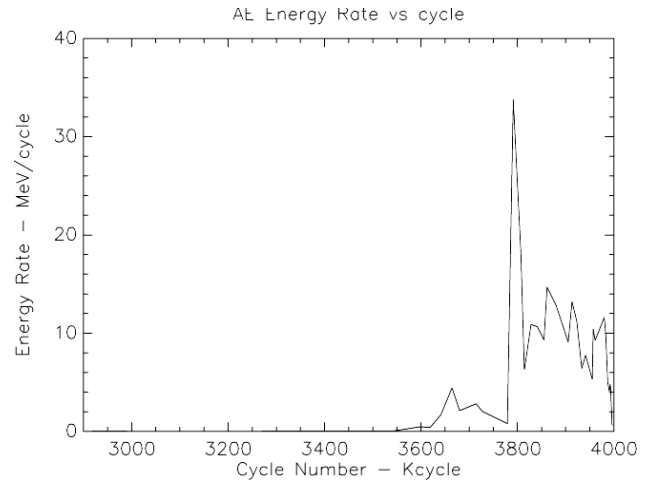Figure 14 – Peak acoustic emission energy versus cycle count.

Figure 15 – Acoustic emission energy rate versus cycle count.

The NASA SHM system was placed entirely in-board from the maximum blade chord. This was the location where the blade had failed previously in static testing.[28] However, and unfortunately, this was not where the blade failed in fatigue.
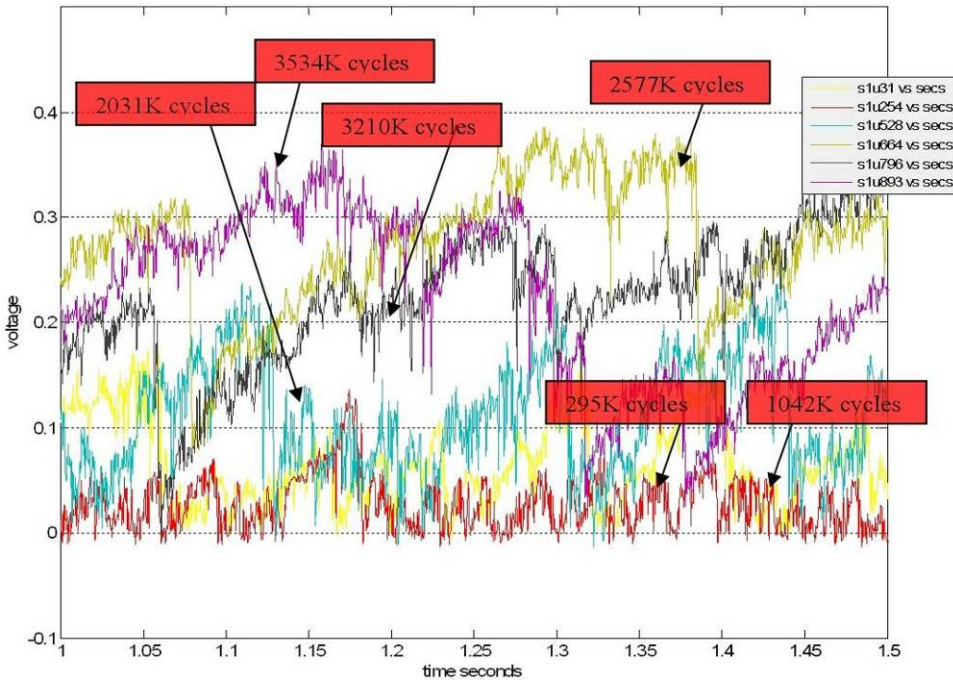

The strains placed on the MFC sensors as the blade was loaded from the UREX mass and the blade movement may have blocked the random input signals from the actuators causing erroneous sensor data. All this resulted in noisy data. However, the analysis to date suggests that the effects of the blade deterioration did affect the boundary conditions enough for sensors CH1 and CH2 to show trends as shown in Figure 16 and Figure 17. The SHM data taken while the blade was cycling has not been analyzed.

Figure 16 – Plots showing the increase in CH1 response as the fatigue cycles increased from 295 kilocycles to 3,534 kilocycles.

That the sensors showed a trend is very encouraging and with improvements to the system and testing methods, and closer placement of the sensors to the failure area, the NASA SHM system appears viable. NASA will perform the data analysis and report the results of the SHM measurements at a later date.
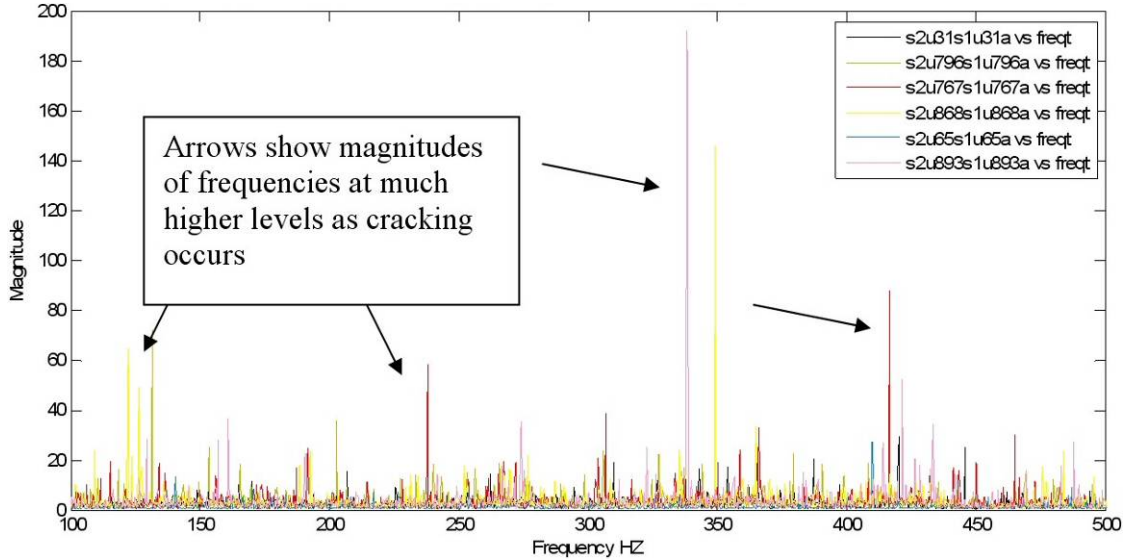

Figure 17 – Plots showing the random input frequency response function for CH2/CH1 showing higher magnitudes as cracking progresses.

The Purdue SHM system did have damage detection sensors mounted on the blade. However, none of the sensors were within 2 meters of the failed location. Summarizing the Purdue analysis to date, the in-plane displacement measurements between the damage and root were found to be sensitive to the crack growth and direction.[46] Of particular interest, the dynamic features of the blade were sensitive to the variations in ambient temperature. Active diagnostics with the method of virtual forces was sensitive to the damage for in-plane measurements following adjustment for thermal effects (see Figure 18). Impact identification was demonstrated with 93% accuracy of the location and within 1.3% accuracy of the magnitude.
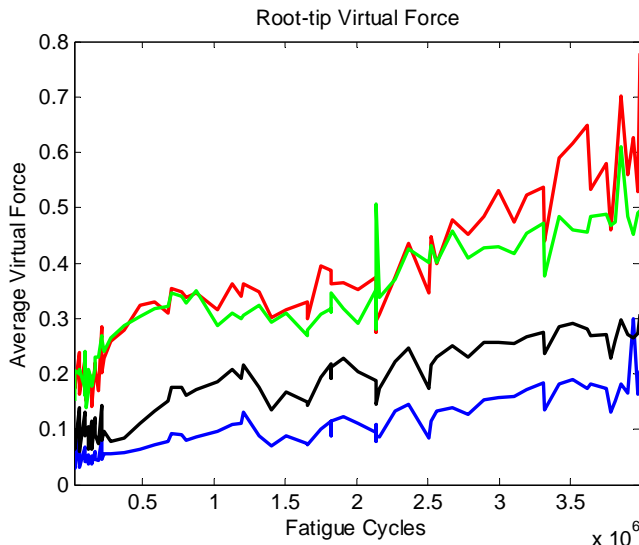

Figure 18 – Root-tip virtual force throughout the fatigue test.

Modal decomposition was an accurate prediction of the excitation mode shapes throughout the test and a practical approach for near-real time load monitoring. Second order harmonics excited by the fatigue system were shown to be on the magnitude of the driving frequency at the tip in the lead-lag and root-tip direction (see Figure 19 and Figure 20). Findings of this test will be instrumental in future development of accelerometer-based wind turbine rotor blade monitoring.

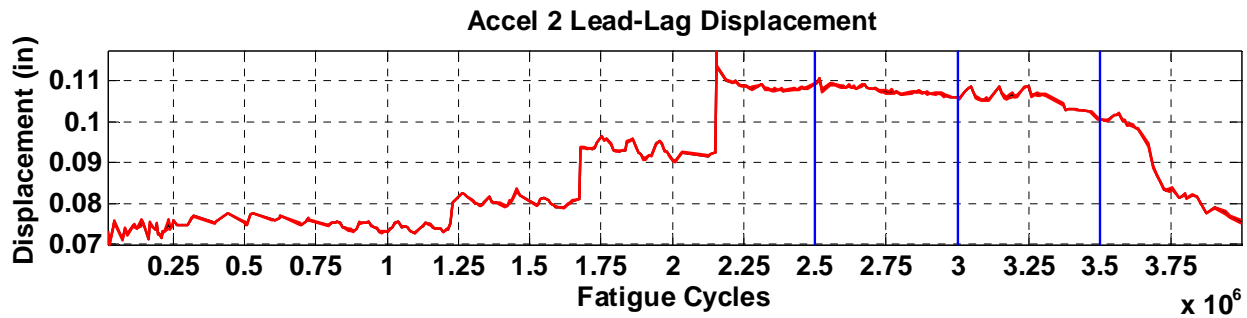More details of the Purdue analysis are given in reference 46.

Accel 2 Lead-Lag Displacement

Figure 19 – The blade lead-lag (edge) tip displacement thoughout the fatigue test.
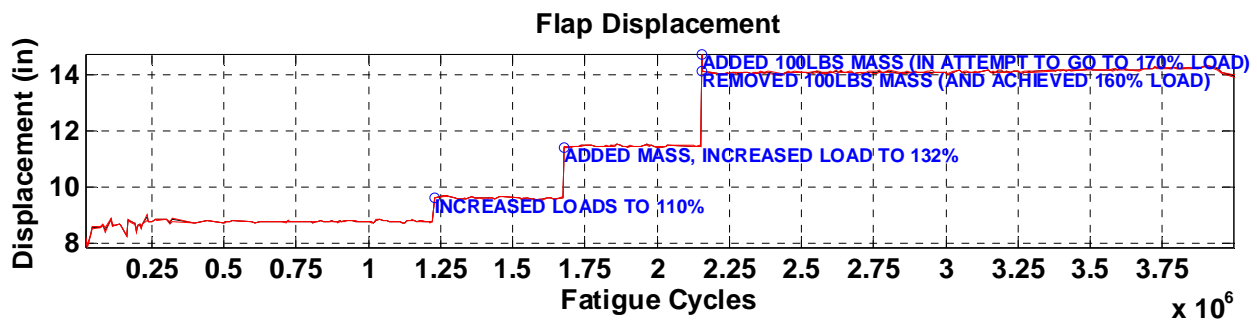
Flap Displacement

Figure 20 – Calculated blade tip displacement during the fatigue test.

Baseline readings of the VT MFC sensors before the fatigue test started showed no peaks and therefore no structural information from 5 k to 60 kHz. However, recording continued throughout the fatigue test, but as expected from the initial baselines, no damage was detected. These results are disappointing considering the VT impedance-based SHM system showed the ability to detect damage on several feasibility tests on a CX-100 wind turbine blade section.[49] However, on the TX-100 blade during the fatigue test the method was insensitive to damage. This is possibly due to the combination of several reasons: using MFC instead of PZT sensors, mounting the sensors on the outside of the blade instead of inside the blade, and likely that the full blade was larger, more massive, and not merely a section and therefore has no boundaries close to the MFC sensors.

The VT SHM system could not record impedances during operation of the fatigue test because the load actuation caused a beat frequency to develop in the impedance data. The UREX had to be stopped to record VT SHM data.
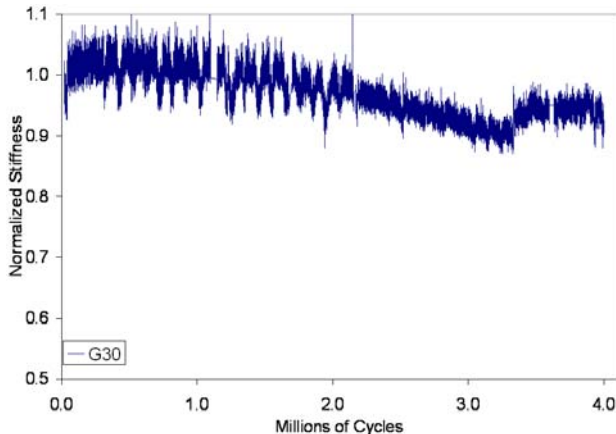

Figure 21 – Normalized response of strain gage G30.

Figure 21 shows the normalized response of strain gage G30 as a function of the fatigue cycle count. The blade can be seen to soften at this location as the cycle count increases. For more information on the strain gage dataset, refer to reference 32.

Figure 22 shows two snap-shots of the photoelastic panel that was on the low pressure, compression, downward facing blade surface over the out-board spar cap termination point at 4.5 meters. Figure 23 shows the thermal gradients around the damage area on the high pressure, tensile, upward facing surface at the 3.8 million cycle count.

Not all the datasets obtained from this fatigue test have been fully analyzed; further results will be forthcoming.
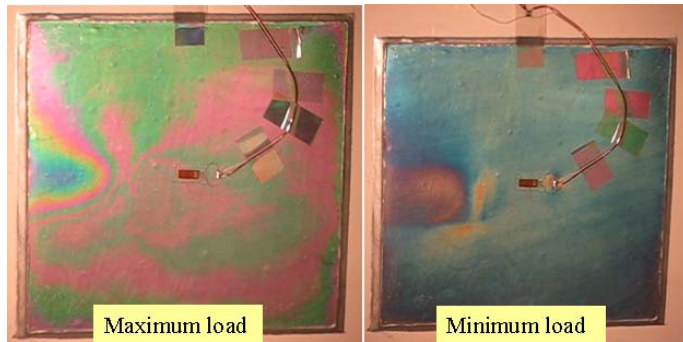
Figure 22 - Two snap-shots (at maximum and minimum fatigue load) of the photoelastic panel on the low pressure, compression, downward facing, blade surface over the spar cap termination point at 4.5 meters. Note the high strain gradients around the termination point of the spar cap.
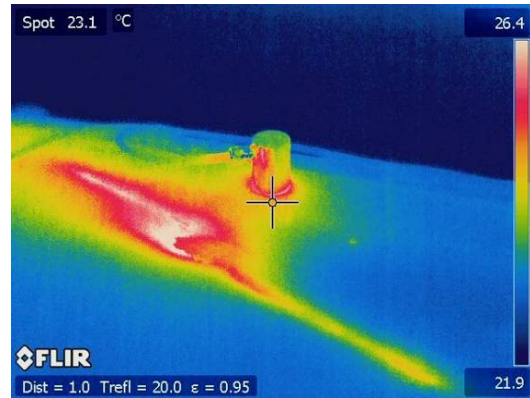

Figure 23 - Infrared thermography image of damage area at 3.8 million fatigue cycles.

5. CONCLUSION

The generation of electricity from wind power is quickly becoming a viable electric utility option. To optimize the operation and maintenance of the wind turbine, additional information is needed from the turbine – the wind turbine structure needs to be smarter. One technology that may provide this intelligence is structural health monitoring. To investigate the potential and issues of using SHM, several SHM techniques were recently implemented and exercised during a fatigue test of a 9 meter TX-100 wind turbine blade, to blade failure, at the NREL/NWTC blade testing facility.

The TX-100 blade failed in fatigue after 4 million cycles on the tensile side of the blade at the spar cap termination point at 4.5 meters. The TX-100 blade fatigue failure mechanism and location was significantly different from a previous static test. Because the fatigue failure mechanism and location was not known before hand, the SHM systems and other diagnostic equipment were not placed in an optimized configuration. The impedance and wave propagation based SHM techniques may have been too far away from the failure location to yield useful results. Further analysis of the datasets is needed to make firm conclusions. There was signal cross-talk interference from other operating active SHM systems; operation of the various SHM and NDT systems had to be choreographed. The SHM results from the restoring force and virtual forces methods were promising. The ability to measure blade tip deflection using an accelerometer was promising. And while not surprising, the structural dynamics of the blade were sensitive to the variations in ambient temperature. These conclusions highlight an inherent challenge in SHM of large structures: detecting damage that often occurs at a small scale while distributing an array of sensors wide enough to monitor the entire structure.

The diversity of materials in a composite wind turbine blade resulted in challenging acoustic properties for AE NDT. The acoustic velocities were highly anisotropic, and the acoustic energy attenuation was comparatively high resulting in sensor separation of 0.4 meters or less. This resulted in increased uncertainty in locating the AE events. However, the AE NDT system did detect significant AE events early in the test and therefore was a very informative diagnostic tool during the wind turbine blade test.

Much work still remains to determine which SHM technique is best suited for a particular wind turbine application, how the SHM technique should be incorporated in a reliable and cost-effective manner, and how to effectively use the information that such SHM techniques produce to make decisions that impact turbine operation.

6. ACKNOWLEDGMENTS

REFERENCES

[1]   American Wind Energy Association (AWEA) news highlight: http://www.awea.org/newsroom/releases/AWEA_Market_Release_Q4_011708.html

[2]   American Wind Energy Association 2007 Market Report, January 2008. http://www.awea.org/Market_Report_Jan08.pdf

[3]   European Wind Energy Association (EWEA) news release: http://www.ewea.org/fileadmin/ewea_documents/mailing/PR_040208_2007stats.pdf

[4]   Global Wind Energy Council (GWEC) http://www.gwec.net/

[5]   Ashwill, T.D., "Some Recent Trends & Activities in Turbines and Blades," Sandia National Laboratories 2nd Wind Turbine Blade Workshop, http://www.sandia.gov/wind/bladeworkshop_06.htm, April 2006.

[6]   American Wind Energy Association (AWEA) news release: http://www.awea.org/newsroom/releases/Wind_Power_Capacity_012307.html

[7]   Sutherland, H.J.; Musial, W., "The Application of Non-Destructive Techniques to the Testing of a Wind Turbine Blade" Proceedings, *WindPower 93*, AWEA, Washington, D.C., 1993.

[8]   Sutherland, H.; Beattie, A.; Hansche, B.; Musial, W.; Alread, J.; Johnson, J. and Summers, M., "The Application Of Non-Destructive Techniques to the Testing of a Wind Turbine Blade," SAND93-1380, Sandia National Laboratories, Albuquerque, NM, June 1994. http://infoserve.library.sandia.gov/sand_doc/1993/931380.pdf

[9]   James, George, "Development of Structural Health Monitoring Techniques using Dynamics Testing," SAND96-0810, Sandia National Laboratories, Albuquerque, NM, March 1996. http://infoserve.library.sandia.gov/sand_doc/1996/960810.pdf

[10]   Sundaresan, M.J.; Schulz, M.J.; and Ghoshal, A., "Structural Health Monitoring Static Test of a Wind Turbine Blade," NREL/SR-500-28719, North Carolina A&T State University Report for NREL, Golden, CO, March 2002. http://www.nrel.gov/wind/pdfs/40089.pdf

[11]   Farrar, Charles R.; Worden, Keith; Todd, Michael D. ; Park, Gyuhae; Nichols, Jonathon; Adams, Douglas E.; Bement, Matthew T.; Farinholt, Kevin "Nonlinear System Identification for Damage Detection," LA-14353, Los Alamos National Laboratories, Los Alamos, NM, November 2007. http://www.lanl.gov/projects/ei/pdf_files/LA_14353_NonlinearReport.pdf

[12]   American Wind Energy Association (AWEA) publication: http://www.awea.org/pubs/factsheets/EconomicsOfWind-Feb2005.pdf

[13]   C.-H. Ong and S. W. Tsai, "The Use of Carbon Fibers in Wind Turbine Blade Design: A SERI-8 Blade Example," SAND2000-0478, Sandia National Laboratories Contractor Report, March 2000. http://infoserve.library.sandia.gov/sand_doc/2000/000478.pdf

[14]   Ashwill, T, and Laird, D, "Concepts to Facilitate Very Large Blades," Proceedings, ASME/AIAA Wind Energy Symposium, Reno, NV, 2007. http://www.sandia.gov/wind/asme/AIAA-2007-0817.pdf

[15]   Berry, Derek and Lockard, S., "Innovative Design Approaches for Large Wind Turbine Blades Final Report," SAND2004-0074, Sandia National Laboratories, Albuquerque, NM, May 2004. http://www.sandia.gov/wind/other/040074.pdf

[16]   Global Energy Concepts, LLC, 1809 7th Avenue, Suite 900, Seattle, WA 98101, (206) 387-4200.

[17]   Dynamic Design Engineering, Inc., 123 C St., Davis CA, (530) 753-7961.

[18]   MDZ Consulting, 601 Clear Lake Road, Clear Lake Shores, Texas 77565, (713) 334-5681.

[19]   TPI Composites, Inc., 373 Market Street, P.O. Box 328, Warren, RI 02885-0367, (401) 247-4010.

[20]   Berry, D., "Design of 9-meter Carbon-Fiberglass Prototype Blades: CX-100 and TX-100," SAND2007-0201, Sandia National Laboratories, Albuquerque, NM, September 2007.

[21]   Jones, P.L.; Sutherland, H.J., Neal, B.A., "LIST/BMI Turbines Instrumentation and Infrastructure," SAND2001-1642, Sandia National Laboratories, Albuquerque, NM, June 2001. http://infoserve.library.sandia.gov/sand_doc/2001/011642.pdf

[22]   P. S. Veers, G. Bir and D. W. Lobitz, "Aeroelastic Tailoring in Wind-Turbine Blade Applications," Proceedings, Windpower '98 Meeting, pp. 291-304.

[23]   Lobitz, D. and Veers, P., "Aeroelastic Behavior of Twist-coupled HAWT Blades," ASME/AIAA Wind Energy Symposium, Reno, NV, 1998, pp. 75-83.

[24] Lobitz, D. and Laino, D., "Load Mitigation with Twist-coupled HAWT Blades," ASME/AIAA Wind Energy Symposium, Reno, NV, 1999, pp. 124-134.

[25] D. Lobitz, P. S. Veers and D. J. Laino, "Performance of Twist-Coupled Blades on Variable Speed Rotors," Proceedings, ASME/AIAA Wind Energy Symposium, Reno, NV, 2000, pp. 404-412.

[26] D. W. Lobitz et al., "The Use of Twist-Coupled Blades to Enhance the Performance of Horizontal Axis Wind Turbines," SAND2001-1303, May 2001. http://infoserve.library.sandia.gov/sand_doc/2001/011303.pdf

[27] D. Griffin, "Evaluation of Design Concepts for Adaptive Wind Turbine Blades," SAND2002-2424, Sandia National Laboratories Contractor Report, August 2002.

[28] Paquette, Joshua; van Dam, Jeroen; Hughes, Scott, "Structural Testing of 9 m Carbon Fiber Wind Turbine Research Blades," AIAA-2007-816, *45th AIAA Aerospace Sciences Meeting and Exhibit*, Reno, NV, 2007.

[29] Paquette, J; Griffith, D.T., "Development of Validated Blade Structural Models," AIAA-2008-1297, *46th AIAA Aerospace Sciences Meeting and Exhibit*, Reno, NV, 2008.

[30] National Renewable Energy Laboratory / National Wind Technology Center, http://www.nrel.gov/wind/

[31] National Renewable Energy Laboratory, http://www.nrel.gov/

[32] Paquette, J.; Hughes, S.; van Dam, J.; Johnson, J., "Fatigue Testing of 9 m Carbon Fiber Wind Turbine Research Blades," AIAA-2008-1350, *46th AIAA Aerospace Sciences Meeting and Exhibit*, Reno, NV, 2008.

[33] Sutherland, H.J., "On the Fatigue Analysis of Wind Turbines," SAND99-0089, Sandia National Laboratories, Albuquerque, NM, June 1999. http://www.prod.sandia.gov/cgi-bin/techlib/access-control.pl/1999/990089.pdf

[34] Physical Acoustics Corp., 195 Clarksville Road Princeton Jct, NJ 08550, 609-716-4000, http://www.pacndt.com/

[35] Dr. Alan Beattie, PAC AE NDT consultant, 515-292-2566, agbames@earthlink.net

[36] Dr. Adrian Pollock, Physical Acoustics Corporation, 195 Clarksville Road, Princeton Jct, NJ 08550, 609-716-4006, apollock@pacndt.com

[37] Rudy Werlink, Lead Project Engineer, 5403 OSB, Mail Stop NEF7, NASA, Kennedy Space Center, FL 32899, (321) 861-7327, Rudolph.J.Werlink@nasa.gov

[38] Zayas, Jose R.; Paquette, Joshua; Werlink, Rudolph J., "Evaluation of NASA PZT Sensor/Actuator for Structural Health Monitoring of a Wind Turbine Blade," Conference paper AIAA 2007-1020, 45th AIAA Aerospace Sciences Meeting and Exhibit, Reno, NV, 2007.

[39] Smart Material Corp., 1990 Main Street, Suite 750, Sarasota, FL 34236. 941-870-3337 http://www.smart-material.com/

[40] Berg, D.E.; Rumsey, M.A.; and Zayas, J.R., "Hardware and Software Developments for the Accurate Time-Linked Data Acquisition System", *2000 ASME Wind Energy Symposium*, 2000, p. 306.

[41] Berg, D.E., and Zayas, J.R., "Accurate Time-Linked Data Acquisition System Field Deployment and Operational Experience", *2001 ASME Wind Energy Symposium*, 2001, p. 153.

[42] Zayas, J.; P. Jones, J.; Ortiz-Moyet, "Accurate GPS Time-Linked Data Acquisition System (ATLAS II) User's Manual", SAND2004-0481, Sandia National Laboratories, Albuquerque, NM, February 2004. http://www.prod.sandia.gov/cgi-bin/techlib/access-control.pl/2004/040481.pdf.

[43] Jonathan White, Graduate Research Assistant, Department of Mechanical Engineering, 140 South Martin Jischke Dr., Purdue University, West Lafayette, IN 47907-2031. https://engineering.purdue.edu/~white69/

[44] Professor Douglas Adams, Purdue University, School of Mechanical Engineering, Ray W. Herrick Laboratories, 140 S. Intramural Drive, West Lafayette, IN 47907-2031, (765) 496-6033, deadams@purdue.edu http://widget.ecn.purdue.edu/~FEND2

[45] Ray W. Herrick Laboratories, School of Mechanical Engineering, Purdue University, https://engineering.purdue.edu/Herrick/index.html

[46] White, J.; Adams, D.; Rumsey, M.; van Dam, J.; Hughes, S., "Impact, Loading and Damage Detection in Carbon Composite TX-100 Wind Turbine Rotor Blade," AIAA-2008-1349, *46th AIAA Aerospace Sciences Meeting and Exhibit*, Reno, NV, 2008.

[47] Corey Pitchford, Graduate Research Assistant, Center for Intelligent Material Systems and Structures, Department of Mechanical Engineering, 310 Durham Hall, Mail Code 0261, Virginia Polytechnic Institute and State University, Blacksburg, VA 24061. http://www.cimss.vt.edu/

[48] Professor Daniel Inman, Center for Intelligent Material Systems and Structures Department of Mechanical Engineering, 310 Durham Hall, Mail Code 026, Blacksburg, VA 24061, (540) 231-4709, dinman@vt.edu

[49] Pitchford, Corey, "Impedance-Based Structural Health Monitoring of Wind Turbine Blades," Master's Thesis, [Aug. 31, 2007]. http://scholar.lib.vt.edu/theses/available/etd-09062007-140545/